Original Research

Volha Lazouskaya
Lian-Ping Wang
Hui Gao
Xiaoyan Shi
Kirk Czymmek
Yan Jin*

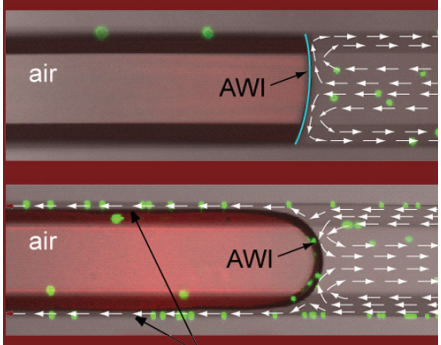

Moving air–water interfaces (AWI) are ubiquitous in soil, such as during imbibition and drainage. A confocal microscope was used to directly visualize moving AWIs in a model unsaturated system. Images derived were used to characterize the role of the AWI in colloid retention and mobilization in unsaturated porous media.

V. Lazouskaya and Y. Jin, Dep. of Plant and Soil Sciences, Univ. of Delaware, Newark, DE 19716; L.-P. Wang, H. Gao, and X. Shi, Dep. of Mechanical Engineering, Univ. of Delaware, Newark, DE 19716; and K. Czymmek, Dep. of Biological Sciences, Univ. of Delaware, Newark, DE 19716. *Corresponding author (yjin@udel.edu).

Vadose Zone J. 10
doi:10.2136/vzj2011.0003
Received 4 Jan. 2011.
Posted online 9 Sept. 2011.

Pore-Scale Investigation of Colloid Retention and Mobilization in the Presence of a Moving Air–Water Interface

A review of current literature shows that considerable uncertainty exists concerning the role of the air–water interface (AWI) in colloid transport in unsaturated porous media. This study aimed to elucidate the mechanisms of colloid mobilization and retention at the AWI in a model dynamic system at the pore scale. The behavior of carboxylate-modified colloids during drainage and imbibition in a microfluidic channel was visualized with a confocal microscope. We found that dispersed hydrophilic colloids did not attach to the AWI under the investigated low ionic strength conditions, while colloids previously attached to the channel walls were mobilized by the contact line, retained at the AWI due to capillary forces, and thus were further transported. The study provides direct experimental evidence on the mechanisms by which colloid attachment to the AWI occurs and emphasizes the involvement of the moving contact line and AWI in colloid mobilization and transport in unsaturated porous media.

Abbreviations: AWI, air–water interface; DLVO, Derjaguin–Landau–Verwey–Overbeek; PMMA, poly(methyl methacrylate).

Colloid transport in soil porous media has been drawing considerable scientific attention due to potentially enhanced transport of contaminants associated with mobile colloids (McCarthy and Zachara, 1989; Saiers and Ryan, 2006; Sen and Khilar, 2006). The interest in colloid transport is intensified by the importance of understanding and predicting microorganism and nanoparticle transport in natural porous media (Jin and Flury, 2002; Ginn et al., 2002; Wiesner et al., 2006). Unsaturated porous media are more complex than saturated porous media due to the presence of the air phase, complicating the flow regime and adding colloid retention sites at the AWI and contact line (where the AWI and the solid meet). The AWI may increase or decrease colloid transport, e.g., by serving as a colloid carrier (e.g., Goldenberg et al., 1989; Wan et al., 1994) or by acting as a dynamic physical barrier (Auset et al., 2005). While some researchers have reported that dispersed colloids deposit on the contact line during AWI movement (e.g., Crist et al., 2005; Lazouskaya and Jin, 2008), others have emphasized the role of a moving (i.e., nonstationary) AWI in mobilizing colloids from the surfaces of porous media (e.g., Saiers et al., 2003; Cheng and Saiers, 2009; Bridge et al., 2009). Despite recent progress, conceptual disagreements on retention mechanisms at the AWI remain (Wan and Tokunaga, 1997; Crist et al., 2004, 2005; Wan and Tokunaga, 2005; Steenhuis et al., 2005), which stem from distinguishing colloid retention mechanisms at the AWI and contact line. Therefore, the occurrence of multiple processes involving colloids and the presence and movement of the AWI requires further evaluation. Moreover, it appears that retention of colloids at the AWI and contact line are closely related and therefore need to be jointly evaluated.

The dynamic nature of soil processes implies the need to consider hydrodynamic processes. For example, it has been shown that physicochemical and hydrodynamic processes are coupled in governing colloid behavior in porous media (Yao et al., 1971; Rajagopalan and Tien, 1976; Johnson et al., 2007; Torkzaban et al., 2007, 2008), with hydrodynamic effects dominating bulk transport and physicochemical effects controlling the interactions of colloids with the interfaces (e.g., the solid–water interface, the AWI, and the contact line). Due to the complexity of colloid transport and retention processes in soil, a considerable portion of colloid transport research has been conducted using pore-scale systems allowing direct visualization of colloid transport and retention (Ochiai et al., 2006). To date, most pore-scale and micromodel studies have focused predominantly on colloid

retention mechanisms affected by solution chemistry (e.g., Wan and Wilson, 1994; Sirivithayapakorn and Keller, 2003b; Crist et al., 2004, 2005; Chen and Flury, 2005; Zevi et al., 2005; Gao et al., 2006). Several have reported on the hydrodynamic behavior of colloids at the pore scale in saturated systems (e.g., Sirivithayapakorn and Keller, 2003a; Auset and Keller, 2004; Baumann and Werth, 2004), but comparably few in unsaturated systems (Gao et al., 2006; Lazouskaya et al., 2006; Lazouskaya and Jin, 2008).

In pore-scale studies focusing on unsaturated colloid transport, the air phase was introduced in a number of ways: as mobile and trapped air bubbles (Wan and Wilson, 1992, 1994; Sirivithayapakorn and Keller, 2003b; Chen and Flury, 2005; Gao et al., 2006), by using open systems (Crist et al., 2004, 2005; Zevi et al., 2005; Lazouskaya et al., 2006; Lazouskaya and Jin, 2008), and by using two-phase flows (Wan and Wilson, 1993; Lazouskaya and Jin, 2008; this study). The different geometries and hydrodynamics of each system were designed to model different AWI configurations in unsaturated porous media. Perhaps due in part to the lack of consistent experimental protocols or the different emphases placed in different studies, a complete understanding of colloid retention at the AWI is pending. For example, while some researchers observed stable retention of colloids at the AWI (e.g., Wan and Wilson, 1994; Gao et al., 2006), others questioned such retention (e.g., Chen and Flury, 2005; Lazouskaya and Jin, 2008).

In addition to retention of dispersed colloids, interactions of in situ or attached colloids with a moving AWI and consequent mobilization due to capillary forces have been of considerable interest in the colloid transport literature (e.g., El-Farhan et al., 2000; Saiers et al., 2003; Zhuang et al., 2007; Shang et al., 2008, 2009; Sharma et al., 2008a,b; Cheng and Saiers, 2009; Bridge et al., 2009). Several field and laboratory column studies have shown that colloid mobilization occurs during both drainage and imbibition events and depends on the irrigation pattern (e.g., flow rate and number of AWI passages) (El-Farhan et al., 2000; Zhuang et al., 2007; Shang et al., 2008). Extensive research investigating colloid removal by an AWI from surfaces (Leenaars and O'Brien, 1989; Noordmans et al., 1997; Gómez Suárez et al., 1999a,b, 2001a,b; Sharma et al., 2008b) provides valuable information on parameters that define colloid mobilization; however, direct colloid-scale observation of this process has not been reported. Moreover, many discussions on colloid mobilization have emphasized the role of the AWI, but failed to point out that mobilization in fact takes place on the contact line. Therefore, we propose to use the term *front*, which includes the action of both the AWI and contact line in colloid mobilization.

The problem of a moving contact line has been extensively discussed in the mathematics and engineering literature (e.g., Pomeau, 2002; Shikhmurzaev, 2006; Fuentes and Cerro, 2007). Numerous theoretical and experimental studies of hydrodynamics in the contact line region and on two-phase flow in circular and square capillaries have been conducted (e.g., Hoffman, 1975; Dussan, 1977; Mumley et al., 1986a,b; Ichikawa et al., 1994; Taha and Cui, 2006). Karnis and Mason (1967) and Yamaguchi et al. (2009) observed the movement of particles near the AWI during two-phase flow in circular tubes and reported accumulation of particles close to the AWI, which was attributed to hydrodynamic interactions. To the best of our knowledge, however, more specific interactions of colloid-size particles (<10 μm) in such systems, especially at the microscopic scale, have not been systematically studied.

In this study, we used a microfluidic channel with an angular (trapezoidal) cross-section to represent a soil capillary (Lazouskaya and Jin, 2008). A moving AWI was created as the phase boundary of two-phase flow in the channel and visualized with a confocal microscope. With this system, we aimed to investigate colloid behavior in the vicinity of a moving AWI and contact line. Both advancing and receding AWIs and contact lines (corresponding to imbibition and drainage fronts, respectively) were considered, and additional emphasis was placed on evaluating the flow field in the interfacial regions and its role in colloid retention and mobilization. In addition, through direct observation, information on the occurrence and interplay of several concurrent mechanisms involving both dispersed and attached colloids was obtained.

Materials and Methods

We used yellow-green fluorescent carboxylate-modified polystyrene microspheres, which have an average diameter of 500 nm and a particle density of 1055 kg m^{-3} (F8813, Molecular Probes, Eugene, OR). All colloid suspensions were prepared by dispersing the microspheres in deionized (DI) water to final concentrations of 2 and 4 mg L^{-1}, or 2.9×10^7 and 5.8×10^7 particles mL^{-1}, respectively (4 mg L^{-1} was used in some experiments to observe more colloids in the images). The colloid zeta potential in DI water (at pH = 5.4 and ionic strength of 1.5×10^{-6} mol L^{-1}) was measured as -65.6 ± 2.3 mV using a Zetasizer Nano ZS (Malvern Instruments, Westborough, MA). Hückel's approximation was used to determine the zeta potential. This approach is more applicable to colloids with thick electric double layers at the low ionic strength of DI water than the commonly used Smoluchowski's approximation (Ross and Morrison, 1988). According to the classification of Petkov and Denkov (2002), which divides particles into hydrophilic (colloid contact angle $\theta < 30°$), partially hydrophobic ($30° < \theta < 90°$), and hydrophobic ($\theta > 90°$), carboxylate-modified colloids are characterized as hydrophilic. We selected these experimental conditions (i.e., low ionic strength, hydrophilic colloids at low concentration) to assess the effect of a flow field on colloid retention in the two-phase flow system, building on our previous study that focused on the effects of solution ionic strength and surface tension on colloid retention at the AWI (Lazouskaya and Jin, 2008). The small size and low concentration of colloids were chosen to ensure that the gravity effect was negligible and that the presence of the particles had minimal effect on the flow field.

The microfluidic channels (Microfluidic ChipShop, Jena, Germany) used in this study were made of poly(methyl methacrylate) (PMMA) and with a trapezoidal cross-section (with base widths of 42 and 70 μm and height or depth of 20 μm). The length of the channels was 85 mm. The acute angle of the trapezoidal cross-section was 54.7° as shown in Fig. 1A (right). The channels are viewed as angular enclosed capillary tubes. The PMMA is partially hydrophobic, with a static contact angle of ~72° and receding and advancing contact angles of 53 and 79°, respectively (Erbil et al., 1999; Lim et al., 2001; Kaczmarek and Chaberska, 2006). We acknowledge that the high-contact-angle channel material of our model setup is not representative of most natural soil materials, although natural systems exhibit great variability and such contact angles have been reported (e.g., Klitzke and Lang, 2007).

Microscopic observations were made through the optically transparent PMMA base (70 μm) of the channel. The dilute (2 or 4 mg L^{-1}) colloid suspension was pumped through the channel with a syringe pump (PHD 22/2000, Harvard Apparatus, Holliston, MA), and concurrent observation of colloid behavior at the point of interest was made with a confocal microscope (Carl Zeiss Axiovert 200M equipped with LSM 510, Oberkochen, Germany) using a 10× magnification lens. To observe colloid behavior in the interfacial regions, an AWI was created by pumping colloid suspension into an empty (dry) channel and establishing a liquid front. The syringe pump was operated in both infusing and withdrawing modes, thus creating two AWI regimes: liquid phase displacing air phase (imbibition front or advancing AWI and contact line) and air phase displacing liquid phase (drainage front or receding AWI and contact line). Sample confocal images of the imbibition and drainage fronts in the channel are shown in Fig. 1. A notable difference between the two regimes is the presence of residual saturation in the channel corners following movement of the drainage front, which is shown schematically in the cross-section in Fig. 1B. The range of flow rates used at different stages of the experiment was from 0 (with the pump stopped) to 0.05 mL h^{-1} (during initial delivery of the colloid suspension to the channel). Most images were recorded at AWI velocities from 5×10^{-6} to 1.3×10^{-5} m s^{-1} (equivalent to flow rates of 2×10^{-5} and 5.2×10^{-5} mL h^{-1}, respectively). The velocity of 10^{-5} m s^{-1} was used as a typical value in calculations. The duration of the experimental observation was between 1 and 3 h.

Images were recorded at a speed of 2 frames s^{-1} with a resolution of 1024 by 130 pixels. Using confocal integrated software (Zeiss LSM) and the advanced imaging software Volocity 3.0.1 (Improvision Inc., Shelton, CT), images were processed to quantify front and colloid velocities, to obtain qualitative information on colloid behavior, and to perform particle tracking. Colloid locations in the z direction, which is perpendicular to the observation, could not be precisely resolved because of the relatively thick imaging optical section (6–7 μm). Due to this limitation and the shallow

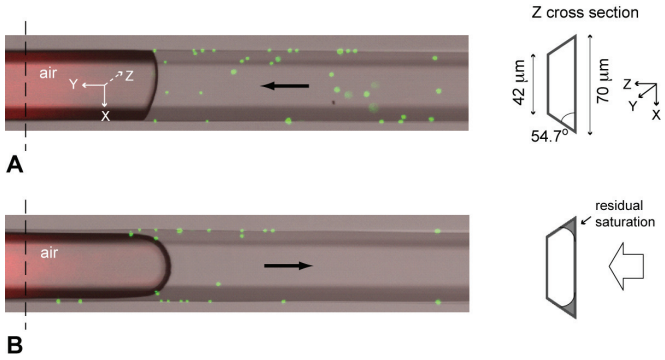

Fig. 1. Images of the microfluidic channel acquired with the confocal microscope and the schematic cross-section in two regimes: (A) imbibition front and (B) drainage front. The dashed lines mark the approximate location of the schematic cross-sections, and the black arrows indicate the flow direction. Note: z cross-section is not shown to scale. The observation occurs through the larger base of the trapezoidal channel, as indicated by the arrow in the schematic cross-section.

channel depth (20 μm) compared with its length and width (Fig. 1), colloid movement in the channel was approximated and treated as two-dimensional. This did not preclude us from distinguishing colloids retained at the AWI from those on the contact line, however, because colloids could be distinguished (i) by the character of their movement because colloids at the AWI were susceptible to Brownian motion while colloids on the contact line were not, and (ii) to a lesser extent by their brightness and overall appearance. Additional information on the optical characteristics of the microscope setup and image acquisition and processing can be found in Lazouskaya et al. (2006) and Lazouskaya and Jin (2008).

During the experiments, colloids both dispersed and attached to the wall were observed. Therefore, all experimental observations were divided into three groups and are considered separately in subsequent discussions: (i) observations of the flow field, (ii) interactions of dispersed colloids with the moving front, and (iii) interactions of attached colloids with the moving front.

Results and Discussion

Observation and Simulation of Flow Field in the Microfluidic Channel

To observe the flow field pattern in the microfluidic channel, we assumed that colloids act as tracer particles, which is valid for colloids not affected by interfacial interactions with the AWI, channel walls, or other colloids. The bulk aqueous flow in the channel was observed at some distance from the AWI (e.g., ~400 μm at a front velocity of 10^{-5} m s^{-1}) and was found to resemble laminar flow with a quasi-parabolic velocity profile; however, the flow field in the vicinity of the AWI was complex. To capture the movement of colloids and the AWI in the same image, the motion of colloids relative to the AWI (as opposed to motion relative to the channel wall) was considered. This representation has been broadly used

in previous two-phase flow studies (e.g., Karnis and Mason, 1967; Dussan, 1977; Shen and Udell, 1985; Yamaguchi et al., 2009). Colloid velocity relative to the AWI was determined as the difference between the absolute colloid velocity (relative to the channel wall) and the AWI velocity.

The observed flow fields, constructed using these relative colloid velocities, for both imbibition and drainage fronts are shown schematically in Fig. 2. As shown, when a colloid approaches the AWI, the direction of its movement relative to the AWI changes due to transition from a far-field quasi-parabolic velocity profile to a nearly uniform velocity profile at the AWI (because of the constant velocity of the AWI). Similar flow patterns have been reported for two-phase flows in larger circular capillaries (e.g., Karnis and Mason, 1967; Dussan, 1977; Ichikawa et al., 1994; Yamaguchi et al., 2009). At lower front velocities, some colloids exhibited random movement and variations in their paths, probably due to Brownian motion, which is notable for the relatively small (500-nm) colloids used in this study. (Additional information on flow patterns for imbibition and drainage fronts can be found in Supplemental Movie 1 and Movie 2, where particle tracking was implemented with Volocity 3.0.1 to visually emphasize the complexity of flow in the vicinity of the AWI).

Simulation of the flow field near a moving AWI and contact line in a two-dimensional channel was performed by Shi et al. (2010) using the multiphase lattice–Boltzmann method of Kang et al. (2004). The simulated flow patterns relative to the moving AWI were consistent with the colloid trajectories observed in the experiments (Fig. 2). For the imbibition front, the relative flow was directed toward the AWI near the center of the channel, but moved away from the AWI near the wall. The opposite was found for the drainage front, where the relative flow near the center moved away from the AWI and into the AWI near the wall. The simulations provided additional details on flow near the AWI and contact line: a stronger transverse flow affecting colloid trajectories was seen for the drainage front than the imbibition front due to a higher front inclination for the former. This transverse flow could generate an enhanced hydrodynamic drag and lift normal to the channel wall and help mobilize previously attached colloids when the drainage front is passing through. This scenario is discussed in more detail below.

Interactions of Dispersed Colloids with Moving Front

Observation of Colloid Movement and Retention

Colloids were observed to closely approach the AWI for both drainage and imbibition fronts at different front velocities, thus creating conditions for colloidal and hydrodynamic interactions with the AWI. At low front velocities, advection of colloids toward the AWI was reduced and occurred due to Brownian motion. At faster front velocities, colloids approached the AWI following the streamlines, shown schematically in Fig. 2, and slid along the AWI before they returned to the bulk solution.

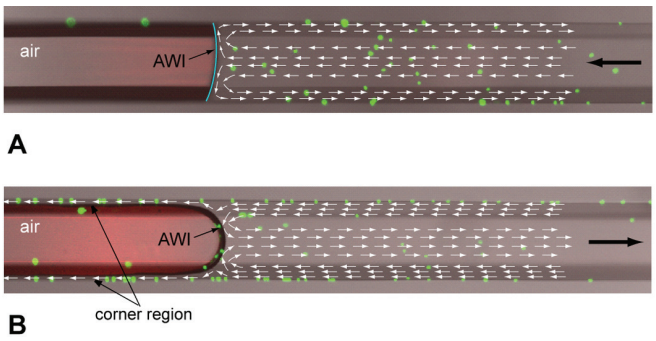

Fig. 2. Schematic flow patterns inferred from observing colloid motion relative to the air–water interface (AWI) shown for (A) imbibition and (B) drainage fronts. White arrows represent the direction of colloid movement relative to the AWI; black arrows on the right indicate the direction of flow and front movement. This is a schematic representation, and the size of arrows shown does not reflect the magnitudes of colloid velocities.

The duration of colloid sliding along an imbibition front varied from 0.5 to 12 s, which was attributed to different flow paths that the colloids followed. For a drainage front, colloid sliding times could not be precisely determined due to frequent advection of the colloids into corner regions (Fig. 2B). Some colloids were observed to reside close to the AWI, probably due to their diminished relative velocities with respect to the AWI (e.g., at convergence or stagnation points; Yamaguchi et al., 2009; Shi et al., 2010). The permanent retention of dispersed colloids at the AWI was not observed for either drainage or imbibition front. This is consistent with the net repulsive interactions between colloids and the AWI under current experimental surface and solution chemistry conditions (Lazouskaya and Jin, 2008).

The presence of residual saturation in the corners following passage of a drainage front allows flow and consequently colloid movement into the corners where colloids move in the direction opposite to the front movement (Fig. 2B). Figure 3 presents an image of a drainage front and a schematic cross-section of the corner; because the exact colloid position in the corner could not be resolved, several possible locations are shown. Most colloids trapped in the corners moved in the bulk residual water (Fig. 3, Position 3). A

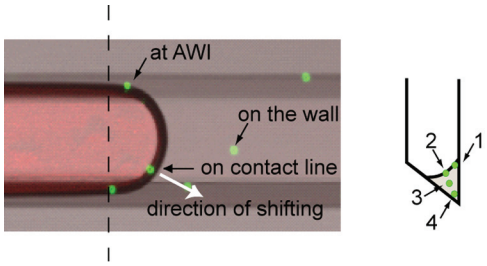

Fig. 3. Confocal image of the air–water interface (AWI) showing observed colloid locations with respect to the drainage front (left) and schematic cross-section showing possible positions of colloids in the corner (right). The dashed line indicates the approximate location of the schematic cross-section.

few also moved in the same direction with the drainage front (Supplemental Movie 3); these colloids were transported either with the AWI of the corner (Fig. 3, Position 2) or on the contact line along the channel wall (Fig. 3, Position 1) and resembled the previously observed reverse flow at the AWI (Lazouskaya et al., 2006). Direct retention of dispersed colloids at the vertex of the corner, although uncommon, was also observed (Fig. 3, Position 4). Such retention is random and could be attributed to wedging (Johnson et al., 2007). Some colloids retained at the vertex were previously retained on the channel wall and were pushed to the corners with the drainage front.

In addition to the AWI, the contact line is another site for potential colloid retention. For a drainage front, corners with residual saturation provide additional regions where colloids are carried with the flow. For an imbibition front, such residual saturation was absent and the contact line in the corner was a preferred location for retention at low front velocities. Colloids moved along the AWI to the contact line, where retention was facilitated by colloid interactions with the solid surface and by film straining (Wan and Tokunaga, 1997). At higher front velocities, however, colloids were diverted from such retention following the streamlines shown in Fig. 2.

Although experimental observations suggest that the hydrodynamic flow pattern plays an imperative role in colloid behavior close to the AWI, colloid forces cannot be ignored and are discussed below, providing a more complete depiction of interactions between dispersed colloids and the AWI.

Equation of Colloid Motion

The problem of particle capture on spherical or cylindrical solid collectors has been extensively discussed in the literature (e.g., Spielman and Goren, 1970; Yao et al., 1971; Spielman, 1977; Schulze, 1984). In this work, the AWI played the role of a collector and, similarly to Nalaskowski et al. (2002), was treated as a solid surface. The problem is additionally complicated with the fact that the AWI is moving. Colloids located in the channel center move in the same direction as the front, which implies that colloid velocities relative to the AWI are smaller than their absolute velocities. Therefore, the relative motion of colloids with respect to the AWI has to be considered.

The equation of motion for a colloid approaching an AWI includes net gravity force, the force of Brownian motion, colloid forces between a particle and the AWI, and hydrodynamic drag force (a detailed description of the forces is provided in the Appendix). These forces calculated using the parameters in Table 1 are plotted in Fig. 4. The figure illustrates the relative magnitudes of the forces as a function of the dimensionless separation distance $H = h/r$ between the colloids and the AWI, where h is separation distance and r is colloid radius. Adopting the convention used in energy calculations, positive and negative signs of a force indicate repulsion and attraction, respectively. As can be inferred from Fig. 4, most

Table 1. Experimental and literature values of parameters used in calculations.

Parameter	Symbol	Value	Source
Temperature	T	298 K (25°C)	measured
Fluid density (water)	ρ_f	997 kg m^{-3}	Pnueli and Gutfinger, 1992
Surface tension (water)	σ	7.2×10^{-2} N m^{-1}	Adamson and Gast, 1997
Viscosity (water)	μ	8.94×10^{-4} Pa s	Pnueli and Gutfinger, 1992
Ionic strength (deionized water)	i	1.5×10^{-6} M	measured
Air-water interface (AWI) zeta potential	ψ_{AWI}	-6.5×10^{-2} V	Graciaa et al., 1995
Colloid zeta potential	ψ	-6.56×10^{-2} V	determined experimentally
Poly(methyl methacrylate) (PMMA) zeta potential	ψ_{PMMA}	-2.5×10^{-2} V	Lubeck et al., 2003
Colloid radius	r	2.5×10^{-7} m	manufacturer, determined experimentally
Colloid density	ρ	1055 kg m^{-3}	manufacturer
Colloid contact angle	θ	~20°	assumed based on value measured for a layer of 1.1-μm colloids (Lazouskaya et al., 2006)
Colloid velocity (typical value)	v	~10^{-5} m s^{-1}	determined experimentally
Front velocity (typical value)	v_{front}	~10^{-5} m s^{-1}	determined experimentally
Fluid velocity	v_f	~10^{-5} m s^{-1}	determined experimentally
Characteristic length (channel dimension)	a	2×10^{-5} m (min.) to 7×10^{-5} m (max.)	manufacturer
PMMA–water contact angles	φ		Erbil et al., 1999; Lim et al., 2001; Kaczmarek and Chaberska, 2006; in agreement with experimental observations
Static		72°	
Receding		53°	
Advancing		79°	

of the forces (with the exception of the randomly directed force of Brownian motion) acting between the colloids and the AWI under the conditions defined in this study are repulsive.

The drag force in Fig. 4 acts on a colloid as it approaches the AWI due to the difference in fluid and colloid velocities and the wall effect (here, the AWI). The drag force acts as a repulsive force because it opposes colloid motion toward the AWI. Although the drag force appears to be long range in the graph, it is expected to be insignificant (e.g., compared with the force of Brownian motion) at a distance of $H = 2$ to 3 (Goren and O'Neill, 1971). The drag force acting on a colloid close to the AWI can be also attractive when a colloid is moving away from the AWI, but that scenario was not considered in Fig. 4.

The Peclet number (Pe) provides information on the relative importance of convection and diffusion (Lenhart and Saiers, 2002) and is defined as $\mathrm{Pe} = rv/D_0$, with $D_0 = kT/6\pi\mu r$, where v is the colloid velocity, D_0 is the diffusion coefficient, k is the Boltzmann constant, T is temperature, and μ is the viscosity. The small Peclet number (Pe = 2.5) points to the importance of Brownian motion, which can be effective in driving a colloid toward the AWI. Whether colloid attachment to an AWI occurs, however, will be determined by the action of colloid forces.

The resulting colloid force under current conditions (hydrophilic colloids and low ionic strength) is repulsive because hydrophobic force does not make a considerable contribution (Lazouskaya and Jin, 2008). Therefore, the retention of dispersed colloids at the AWI is unlikely, and the temporary presence of colloids close to the AWI, reported above, was due to either the action of Brownian motion, flow streamlines in the tangential direction (with less hydrodynamic resistance, as indicated in the Appendix), or the existence of flow stagnation regions (Yamaguchi et al., 2009; Shi et al., 2010). Therefore, knowledge of flow fields in interfacial regions together with an analysis of physicochemical interactions is essential for providing a more complete understanding of colloid behavior close to the AWI.

Interactions of Attached Colloids with Moving Front

Apart from dispersed colloids, colloids attached to the channel walls, AWI, and contact line were present. Most colloids found on channel walls were deposited from the bulk suspension, but some were previously retained and then detached from the contact line. As described above, stable retention of dispersed colloids at the AWI is unlikely. Nevertheless, colloids already retained at the AWI were clearly observed in the experiments, suggesting that they originated not as dispersed colloids from the bulk phase but as a result of mobilization of previously attached colloids from the channel wall. This is true for both drainage and imbibition fronts.

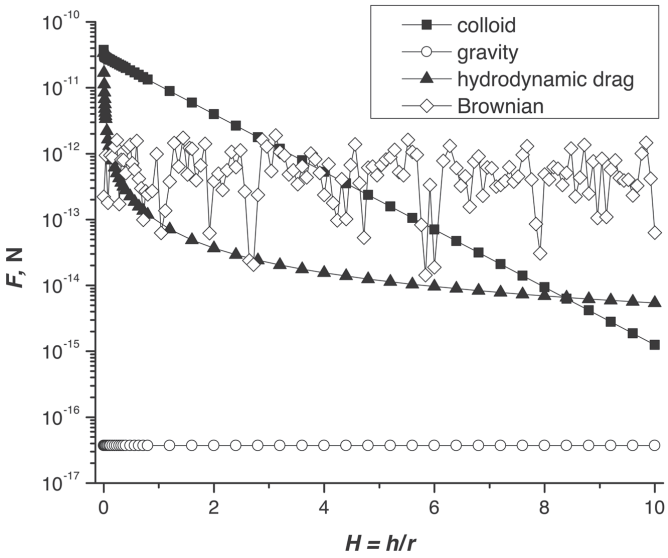

Fig. 4. The magnitudes of forces F (logarithmic scale) acting on a colloid, in the direction normal to the air–water interface (AWI), plotted against the dimensionless separation from the AWI (H). Note: for magnitude comparison, the direction of Brownian motion force has not been accounted for.

After passage of a moving front, several cases of attached colloids were observed, including those (i) mobilized by the contact line and then transported with the AWI (as illustrated in Supplemental Movie 4); (ii) shifted with the front toward the corner region (e.g., moved with the contact line along the wall, as indicated with the white arrow in Fig. 3, and upon the front passage held in Position 1, Fig. 3); (iii) mobilized back into the bulk solution after interacting with the front; and (iv) unaffected on the wall. As the front passes, the behavior of attached colloids is determined by the force balance between colloid, channel wall, and AWI interactions. Depending on the colloid location and attachment conditions, which exhibit a broad distribution at the colloid scale, all of the cases outlined above were observed.

Mechanism of Colloid Mobilization

To explain the observations and differences between mobilizing and shifting the attached colloids by the front (Cases i and ii listed above), the major forces acting on a colloid on the contact line were considered. The positions of colloids relative to the AWI and contact line are shown schematically in Fig. 5: for the drainage front (Fig. 5A), the imbibition front (Fig. 5B), and the drainage front and rough channel surface (Fig. 5C). The forces shown in Fig. 5 include colloid forces between the colloid and the channel wall (PMMA), F_{col}, the drag force imposed by the AWI movement, F_{D}, and the surface tension (capillary) force, F_{σ}.

The force between the colloids and the PMMA surface was estimated similar to colloid–AWI interactions (Lazouskaya and Jin, 2008). Only Derjaguin–Landau–Verwey–Overbeek (DLVO; Derjaguin and Landau, 1941; Verwey and Overbeek, 1948) forces, electrostatic and van der Waals, were included, however, because

the hydrophobic force was found to be unimportant under the current conditions. While the exact surface potential value of PMMA is not known, it was assumed to be −25 mV (Lubeck et al., 2003), and the total colloid interaction force was determined to be on the order of 10^{-10} N or smaller. Experimental observations (e.g., Cases ii and iii) suggest secondary-minimum retention as the probable retention mechanism on the wall. This could not be proved by DLVO calculations, however, which could be due to uncertainty in the PMMA surface potential.

The drag force in the y direction, $F_D = 6\pi\mu r v_{front}$, where v_{front} is the AWI velocity, was determined to be on the order of 10^{-14} N. Also, drag forces on colloid detachment were trivial compared with other forces, as reported previously (Gómez Suárez et al., 1999a; Shang et al., 2008). A transverse component (directed toward the channel center) of the drag force due to the flow field (Fig. 2), which could contribute to colloid mobilization by the drainage front, was not considered in Fig. 5.

The maximum surface tension force in the z and y directions, illustrated in Fig. 5A (drainage front) and 5B (imbibition front), can be determined as (Leenaars, 1988; Noordmans et al., 1997)

Drainage front:

$$F_\sigma^z = -2\pi r\sigma \sin^2\left(\frac{\pi+\theta}{2}\right)\cos\varphi \quad [1]$$

$$F_\sigma^y = -2\pi r\sigma \sin^2\left(\frac{\pi+\theta}{2}\right)\sin\varphi \quad [2]$$

Imbibition front:

$$F_\sigma^z = 2\pi r\sigma \sin^2\left(\frac{\theta}{2}\right)\cos\varphi \quad [3]$$

$$F_\sigma^y = 2\pi r\sigma \sin^2\left(\frac{\theta}{2}\right)\sin\varphi \quad [4]$$

where σ is the surface tension, θ is the colloid contact angle, and φ is the receding (drainage front) or advancing (imbibition front) contact angle of the channel wall. Using the values in Table 1, surface tension force components $F_\sigma{}^z$ and $F_\sigma{}^y$ were determined as -6.6×10^{-8} and -8.6×10^{-8} N, respectively, for a drainage front, and 6.5×10^{-10} and 3.3×10^{-9} N, respectively, for an imbibition front. In both configurations, the surface tension force dominates colloid and drag forces. In particular, the y component of the surface tension force dominates all other forces in the (negative) y direction, explaining the observed shifting of the particle along the channel surface (Case ii).

Colloid transfer from the contact line to the AWI (Case i) cannot be predicted from the analysis above (Fig. 5A and 5B) due to the absence of a governing repulsive force in the z direction. At the same time, surface irregularities may result in regions of lower adhesion than predicted theoretically (Bowen and Doneva, 2002; Butt et al., 2005). Therefore, transfer to the AWI will occur when colloid forces are too weak to maintain colloid attachment to the wall and are unable to resist hydrodynamic disturbances. Although an accurate description of hydrodynamics in the contact line region has not yet been achieved, there have been reports of a rolling motion in close proximity to an advancing interface (e.g., Dussan, 1979; de Gennes, 1985; Pismen, 2002). The mobile surfactant-free AWI (and therefore colloids on the contact line) is susceptible to any hydrodynamic disturbance (Roizard et al., 1999). Therefore, the dominant surface tension force and complex flow field close to the contact line (Fig. 2), coupled with weaker adhesion to the channel wall, are the plausible causes for the observed colloid mobilization with a moving front (Fig. 5C). (This process is illustrated in Supplemental Movie 4).

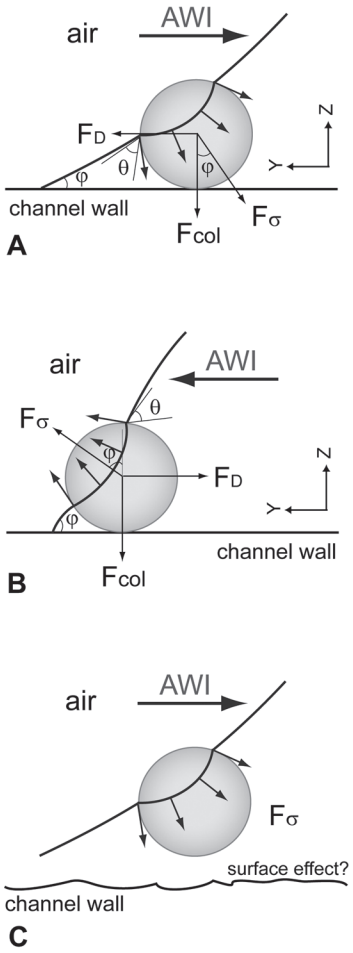

Fig. 5. Drag force (F_D), colloid forces (F_{col}), and surface tension force (F_σ) acting on a particle interacting with (A) a drainage front (contact angle φ = 53°, receding), (B) an imbibition front (φ = 79°, advancing), and (C) a drainage front, illustrated with a possible mechanism of colloid mobilization. The horizontal arrow at the top part of each part indicates the direction of the air–water interface (AWI) movement.

The prerequisite for Cases i and ii is a sufficiently strong attachment of a colloid to the PMMA wall to allow formation of a three-phase contact on a colloid. When colloid–PMMA interactions are not strong enough, repulsive forces between colloids and the AWI will cause mobilization of attached colloids from the wall back into the bulk flow, as observed (Case iii). Regarding Case iv, the stable colloid attachment on the wall probably occurred in the primary energy minimum.

Efficiency of Colloid Mobilization and Transport with Moving Front

Colloids attached to the AWI can be transported along the channel for long times (at least 45 min as experimentally observed) with both drainage and imbibition fronts. This form of transport can be limited, however, for a number of reasons including the finite area of the AWI available for carrying colloids and possible detachment of colloids from the front during its movement.

For the drainage front, no detachment of colloids (i.e., redeposition to the wall or return to the solution) was observed from the front. Due to the presence of residual saturation in the corners, however, colloids at the AWI could be advected there and transported into the corner (Fig. 3, Position 2). As shown with the streamlines in Fig. 2B, flow in the corners occurs in the direction opposite to the front movement. Further colloid behavior in the corners includes retention on the contact line (e.g., Fig. 3, Position 1), retention in the corner as a result of drying (Fig. 3, Position 4), and remobilization following an imbibition event (e.g., Auset et al., 2005). Despite these limitations due to residual saturation, transport with the drainage front under the investigated conditions is a feasible mechanism. (Colloid mobilization and transport with the AWI can be viewed in Supplemental Movie 5 and Movie 6, showing increasing colloid concentration at the moving AWI with time).

Colloid redeposition from the front to the channel wall was a common feature observed for imbibition. This difference from the drainage front can be explained by comparing the surface tension forces acting on colloids in Fig. 5A and 5B. The components of the surface tension force for an imbibition front are weaker than for a drainage front in both z and y directions and are similar to the colloid force in the z direction. The observation of the flow field near the AWI (Fig. 2) also supports higher mobilization with the drainage front: the relative transverse flow in the liquid phase for a drainage front is directed from the wall to the center and contributes to colloid detachment while it is opposite for an imbibition front.

It should be noted, however, that direct comparison of colloid mobilization and transport between drainage and imbibition fronts is not possible due to unequal initial conditions: the drainage front interacts with a greater number of colloids deposited in the liquid phase while the imbibition front interacts with fewer colloids previously deposited and left on the surface after drainage (interaction in the air phase). Also, it is important to emphasize that colloid and surface contact angles serve as variables in Eq. [1–4] and therefore can affect the value and direction of the surface tension force and overall force balance in each particular situation. Therefore, the mobilization efficiency of the drainage and imbibition fronts will differ for different colloid and surface properties.

Another scenario of imbibition front behavior, which was not considered in this study, includes imbibition front movement in a previously wet channel. Hydrophilic porous media will commonly have a thin film of water on the grain surfaces. While surface tension forces play a similar role as in initially dry channels, mobilization of colloids previously retained in regions of residual saturation and liquid films will occur with the imbibition front and may be considerable (Saiers and Lenhart, 2003; Auset et al., 2005; Shang et al., 2008). Our observations, which are specific for these experimental conditions, do not indicate a strong effect of residual thin films on colloid mobilization with a drainage front; however, the presence of residual films, their thickness, and colloid size need to be considered in assessing colloid mobilization under different conditions.

Summary and Conclusions

We investigated mechanisms of colloid retention and mobilization associated with imbibition and drainage fronts by direct observation of colloid behavior in the vicinity of a moving AWI and contact line at the interface or pore scale. Processes similar to those observed in this study can also take place in unsaturated porous media. The complex flow pattern observed in the proximity of the AWI in a trapezoidal channel can be extended to other angular channel geometries, including irregular soil capillaries. Both experimental results and theoretical analyses showed that retention of dispersed colloids at the AWI under the investigated conditions is unlikely. Retention of dispersed colloids can occur on the contact line (in particular, for an imbibition front at low velocities) and in angular corners of capillaries.

The key contribution of a moving contact line to colloid transport is mobilization of attached colloids, which can transfer to the AWI, where they are retained and further transported. Overall, mobilization and transport efficiency of imbibition or drainage fronts can be affected by colloid and surface contact angles and the initial number of colloids available for mobilization. In addition, the presence of residual water films may also affect mobilization, but this phenomenon was not investigated in this work.

Due to the potentially high AWI area associated with moving fronts, the roles of moving contact lines and AWIs in colloid mobilization and transport should be considered in future experimental work and in modeling colloid transport under transient unsaturated conditions.

Appendix

Force Formulation for Equation of Colloid Motion

The equation of motion for a colloid approaching an AWI includes the hydrodynamic drag force, the force of Brownian motion, the net gravity force, and colloid forces between a particle and the AWI. The equation can be written as (Nguyen and Schulze, 2004; Johnson et al., 2007)

$$m\frac{d\vec{v}}{dt}=-\frac{1}{2}m_f\frac{d\vec{v}}{dt}+\vec{F}_D+\vec{F}_{col}+\vec{F}_{Br}+\vec{F}_G \quad [A1]$$

where the first term on the right-hand side is the added-mass term, $\vec{F}_D$ is the drag force, $\vec{F}_{Br}$ is the force due to Brownian diffusion, $\vec{F}_G$ is the net gravity force, and $\vec{F}_{col}$ represents colloid forces including electrostatic (F_{el}), van der Waals (F_{vdW}), and hydrophobic (F_h) forces, which are calculated according to the extended DLVO theory (Derjaguin and Landau, 1941; Verwey and Overbeek, 1948; Yoon and Mao, 1996); m is the particle mass, m_f is mass of the fluid, the volume of which equals the volume of the particle, and $\vec{v}$ is the particle velocity. Figure A1 illustrates a colloid approaching the AWI and the normal and tangential directions relative to the AWI (Spielman and Goren, 1970).

In the normal direction, a drag force F_D^n emerges due to the difference in colloid and fluid velocities near the AWI and can be determined by superposition of the two cases, i.e., a moving colloid in quiescent fluid and a stationary colloid in undisturbed flow normal to the AWI:

$$F_D^n=6\pi\mu r\left[\frac{v_n-v_{front}\cos\alpha}{F_1}-(u_n-v_{front}\cos\alpha)F_2\right] \quad [A2]$$

where $(v_n - v_{front}\cos\alpha)$ and $(u_n - v_{front}\cos\alpha)$ are colloid and fluid relative velocities in the normal direction, respectively; F_1 and F_2 are universal hydrodynamic functions of the dimensionless separation H between the particle and the surface (AWI). Functions F_1 and F_2 have been obtained by Brenner (1961) and by Goren and O'Neill (1971), respectively, to account for short-range hydrodynamic interactions close to a surface (wall). Function F_1 can be specified as a ratio of the particle velocity under an applied force (normal to the collector) to the particle velocity under the same force away from the collector (Spielman, 1977) and F_2 as a ratio of the force exerted by the flow at the particle (normal to the collector) to the force exerted on the particle in a uniform flow away from the collector (Spielman, 1977; Russel et al., 1989). In this study, approximate expressions for F_1 and F_2 provided by Warszynski (2000) were used, which are expressed as

$$F_1(H)=\frac{19H^2+4H}{19H^2+26H+4} \quad [A3]$$

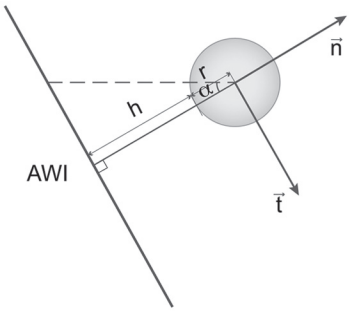

Fig. A1. Geometry of a colloid approaching the air–water interface (AWI); h is the separation distance, r is the colloid radius, α is the angle between the direction of colloid movement and the normal to the AWI, and $\vec{n}$ and $\vec{t}$ are the directions normal and tangential to the AWI.

and

$$F_2(H)=1+\frac{1.79}{(0.828+H)^{1.167}} \quad [A4]$$

Expressions for colloid forces $F_{col} = F_{el} + F_{vdW} + F_h$ (acting in the normal direction) were obtained by differentiating the previously used energy expressions (e.g., Lazouskaya et al., 2006; Lazouskaya and Jin, 2008) as $F = -(dV/dh)$, where V is the interaction energy.

The gravity force $\vec{F}_G$ acts in the z direction (perpendicular to the observed area in Fig. A1). Therefore, it does not contribute to colloid approach or attachment to the AWI in the experimental geometrical configuration (and can be regarded as "repulsive"). Moreover, the net gravity force, calculated as $F_G = (4/3)\pi r^3(\rho - \rho_f)g$, where ρ is the colloid density, ρ_f is the fluid density, and g is acceleration due to gravity, has a small value and can be neglected for 500-nm particles.

The force of Brownian motion has a random direction and value and can be modeled as a Gaussian white noise process (Kim and Zydney, 2004; Johnson et al., 2007; Gao et al., 2008). The force of Brownian motion is expressed as $F_{Br} = \delta\sqrt{(12\pi\mu rkT/\Delta t)}$ in each spatial direction, where δ denotes random numbers obeying a normal distribution (with zero mean and unit standard deviation) and Δt is the time step. The choice of Δt is made by accounting for the inertial response time (or momentum relaxation time) of the colloid, expressed as $\tau_p = 2\rho r^2/9\mu$ (Kim and Zydney, 2004; Gao et al., 2008). A time step larger than the inertial response time is usually used to neglect particle inertia (Maniero and Canu, 2006; Johnson et al., 2007). In many practical problems, however, the time step needs to be adjusted to account for the important (e.g., scale-related) changes in the system (Maniero and Canu, 2006; Johnson et al., 2007). In this study, the time step was taken as 6.4×10^{-5} s, similar to that used by Gao et al. (2008) and Shi et al. (2010), based on the similarity of colloid properties and flow velocity.

Similarly, in the tangential direction, corrections to the hydrodynamic components are also necessary due to the collector proximity. Universal functions F_4 and F_3 in the tangential direction, analogous to functions F_1 and F_2 in the normal direction, were computed by Goren and O'Neill (1971). The correction for colloid mobility F_1 (normal) is larger than F_4 (tangential), as is the wall effect in the normal direction (Warszynski, 2000). Another difference from the normal case is that colloid forces do not operate in the tangential direction. Therefore, in this study we limited the estimate of forces and their comparison to the normal direction (Fig. 4).

Acknowledgments

This study was supported by National Research Initiative Competitive Grant no. 2006-02551 from the USDA Cooperative State Research, Education, and Extension Services.

References

Adamson, A.W., and A.P. Gast. 1997. Physical chemistry of surfaces. John Wiley & Sons, New York.

Auset, M., and A.A. Keller. 2004. Pore-scale processes that control dispersion of colloids in saturated porous media. Water Resour. Res. 40:W03503. doi:10.1029/2003WR002800

Auset, M., A.A. Keller, F. Brissaud, and V. Lazarova. 2005. Intermittent filtration of bacteria and colloids in porous media. Water Resour. Res. 41:W09408. doi:10.1029/2004WR003611

Baumann, T., and C.J. Werth. 2004. Visualization and modeling of polystyrol colloid transport in a silicon micromodel. Vadose Zone J. 3:434–443.

Bowen, W.R., and T.A. Doneva. 2002. Atomic force microscopy of membranes. p. 664–681. *In* A.T. Hubbard (ed.) Encyclopedia of surface and colloid science. Marcel Dekker, New York.

Brenner, H. 1961. The slow motion of a sphere through a viscous fluid towards a plane surface. Chem. Eng. Sci. 16:242–251. doi:10.1016/0009-2509(61)80035-3

Bridge, J.W., A.L. Heathwaite, and S.A. Banwart. 2009. Measurement of colloid mobilization and redeposition during drainage in quartz sand. Environ. Sci. Technol. 43:5769–5775. doi:10.1021/es900616j

Butt, H.-J., B. Cappella, and M. Kappl. 2005. Force measurements with the atomic force microscope: Technique, interpretation and applications. Surf. Sci. Rep. 59:1–152. doi:10.1016/j.surfrep.2005.08.003

Chen, G., and M. Flury. 2005. Retention of mineral colloids in unsaturated porous media as related to their surface properties. Colloids Surf. A 256:207–216. doi:10.1016/j.colsurfa.2005.01.021

Cheng, T., and J.E. Saiers. 2009. Mobilization and transport of in situ colloids during drainage and imbibition of partially saturated sediments. Water Resour. Res. 45:W08414. doi:10.1029/2008WR007494

Crist, J.T., J.F. McCarthy, Y. Zevi, P. Baveye, J.A. Throop, and T.S. Steenhuis. 2004. Pore-scale visualization of colloid transport and retention in partly saturated porous media. Vadose Zone J. 3:444–450.

Crist, J.T., Y. Zevi, J.F. McCarthy, J.A. Throop, and T.S. Steenhuis. 2005. Transport and retention mechanisms of colloids in partially saturated porous media. Vadose Zone J. 4:184–195.

de Gennes, P.G. 1985. Wetting: Statics and dynamics. Rev. Mod. Phys. 57:827–863. doi:10.1103/RevModPhys.57.827

Derjaguin, B.V., and L. Landau. 1941. Theory of the stability of strongly charged lyophobic sols and the adhesion of strongly charged particles in solutions of electrolytes. Acta Physicochim. URSS 14:633–662.

Dussan, E.B., V. 1977. Immiscible liquid displacement in a capillary tube: The moving contact line. AIChE J. 23:131–133. doi:10.1002/aic.690230122

Dussan, E.B., V. 1979. On the spreading of liquids on solid surfaces: Static and dynamic contact lines. Annu. Rev. Fluid Mech. 11:371–400. doi:10.1146/annurev.fl.11.010179.002103

El-Farhan, Y.H., N.M. Denovio, J.S. Herman, and G.M. Hornberger. 2000. Mobilization and transport of soil particles during infiltration experiments in an agricultural field, Shenandoah Valley, Virginia. Environ. Sci. Technol. 34:3555–3559. doi:10.1021/es991099g

Erbil, H.Y., G. McHale, S.M. Rowan, and M.I. Newton. 1999. Determination of the receding contact angle of sessile drops on polymer surfaces by evaporation. Langmuir 15:7378–7385. doi:10.1021/la9900831

Fuentes, J., and R.L. Cerro. 2007. Surface forces and inertial effects on moving contact lines. Chem. Eng. Sci. 62:3231–3241. doi:10.1016/j.ces.2007.03.012

Gao, B., J.E. Saiers, and J. Ryan. 2006. Pore-scale mechanisms of colloid deposition and mobilization during steady and transient flow through unsaturated granular media. Water Resour. Res. 42:W01410. doi:10.1029/2005WR004233

Gao, H., J. Han, Y. Jin, and L.-P. Wang. 2008. Modelling microscale flow and colloid transport in saturated porous media. Int. J. Comput. Fluid Dyn. 22:493–505. doi:10.1080/10618560802238259

Ginn, T.R., B.D. Wood, K.E. Nelson, T.D. Scheibe, E.M. Murphy, and T.P. Clement. 2002. Processes in microbial transport in the natural subsurface. Adv. Water Resour. 25:1017–1042. doi:10.1016/S0309-1708(02)00046-5

Goldenberg, L.C., I. Hutcheon, and N. Wardlaw. 1989. Experiments on transport of hydrophobic particles and gas bubbles in porous media. Transp. Porous Media 4:129–145. doi:10.1007/BF00134994

Gómez-Suárez, C., H.J. Busscher, and H.C. van der Mei. 2001a. Analysis of bacterial detachment from substratum surfaces by the passage of air–liquid interfaces. Appl. Environ. Microbiol. 67:2531–2537. doi:10.1128/AEM.67.6.2531-2537.2001

Gómez Suárez, C., J. Noordmans, H.C. van der Mei, and H.J. Busscher. 1999a. Removal of colloidal particles from quartz collector surfaces as stimulated by the passage of liquid–air interfaces. Langmuir 15:5123–5127. doi:10.1021/la981608c

Gómez Suárez, C., J. Noordmans, H.C. van der Mei, and H.J. Busscher. 1999b. Detachment of colloidal particles from collector surfaces with different electrostatic charge and hydrophobicity by attachment to air bubbles in a parallel plate flow chamber. Phys. Chem. Chem. Phys. 1:4423–4427. doi:10.1039/a905156b

Gómez-Suárez, C., H.C. van der Mei, and H.J. Busscher. 2001b. Air bubble-induced detachment of polystyrene particles with different sizes from collector surfaces in a parallel plate flow chamber. Colloids Surf. A 186:211–219. doi:10.1016/S0927-7757(00)00799-8

Goren, S.L., and M.E. O'Neill. 1971. On the hydrodynamic resistance to a particle of a dilute suspension when in the neighbourhood of a large obstacle. Chem. Eng. Sci. 26:325–338. doi:10.1016/0009-2509(71)83008-7

Graciaa, A., G. Morel, P. Saulner, J. Lachaise, and R.S. Schechter. 1995. The ζ-potential of gas bubbles. J. Colloid Interface Sci. 172:131–136. doi:10.1006/jcis.1995.1234

Hoffman, R.L. 1975. A study of the advancing interface: I. Interface shape in liquid–gas systems. J. Colloid Interface Sci. 50:228–241. doi:10.1016/0021-9797(75)90225-8

Ichikawa, N., M. Kawaji, C. Lorencez, and K. Takata. 1994. Flow distribution near interface of capillary flow in a tube using photochromic dye activation method. Microgravity Sci. Technol. 7:156–159.

Jin, Y., and M. Flury. 2002. Fate and transport of viruses in porous media. Adv. Agron. 77:39–102. doi:10.1016/S0065-2113(02)77013-2

Johnson, W.P., X. Li, and G. Yal. 2007. Colloid retention in porous media: Mechanistic confirmation of wedging and retention in zones of flow stagnation. Environ. Sci. Technol. 41:1279–1287. doi:10.1021/es061301x

Kaczmarek, H., and H. Chaberska. 2006. The influence of UV-irradiation and support type on surface properties of poly(methyl methacrylate) thin films. Appl. Surf. Sci. 252:8185–8192. doi:10.1016/j.apsusc.2005.10.037

Kang, Q., D. Zhang, and S. Chen. 2004. Immiscible displacement in a channel: Simulations of fingering in two dimensions. Adv. Water Resour. 27:13–22. doi:10.1016/j.advwatres.2003.10.002

Karnis, A., and S.G. Mason. 1967. The flow of suspensions through tubes: VI. Meniscus effects. J. Colloid Interface Sci. 23:120–133. doi:10.1016/0021-9797(67)90093-8

Kim, M., and A.L. Zydney. 2004. Effect of electrostatic, hydrodynamic, and Brownian forces on particle trajectories and sieving in normal flow filtration. J. Colloid Interface Sci. 269:425–431. doi:10.1016/j.jcis.2003.08.004

Klitzke, S., and F. Lang. 2007. Hydrophobicity of soil colloids and heavy metal mobilization: Effects of drying. J. Environ. Qual. 36:1187–1193. doi:10.2134/jeq2006.0427

Lazouskaya, V., and Y. Jin. 2008. Colloid retention at air–water interface in a capillary channel. Colloids Surf. A 325:141–151. doi:10.1016/j.colsurfa.2008.04.053

Lazouskaya, V., Y. Jin, and D. Or. 2006. Interfacial interactions and colloid retention under steady flows in a capillary channel. J. Colloid Interface Sci. 303:171–184. doi:10.1016/j.jcis.2006.07.071

Leenaars, A.F.M. 1988. A new approach to the removal of sub-micron particles from solid (silicon) substrates. p. 361–372. *In* K.L. Mittal (ed.) Particles on surfaces 1: Detection, adhesion, and removal. Plenum Press, New York.

Leenaars, A.F.M., and S.B.G. O'Brien. 1989. Particle removal from silicon substrates using surface tension forces. Philips J. Res. 44:183–209.

Lenhart, J.J., and J.E. Saiers. 2002. Transport of silica colloids through unsaturated porous media: Experimental results and model comparisons. Environ. Sci. Technol. 36:769–777. doi:10.1021/es0109949

Lim, H., Y. Lee, S. Han, J. Cho, and K.-J. Kim. 2001. Surface treatment and characterization of PMMA, PHEMA, and PHPMA. J. Vac. Sci. Technol. A 19:1490–1496. doi:10.1116/1.1382650

Lubeck, C.R., M.C. Chin, and F.M. Doyle. 2003. Functionalization of a synthetic polymer to create inorganic/polymer hybrid materials. p. 95–104. *In* J.J. Kellar et al. (ed.) Functional fillers and nanoscale minerals: New markets/new horizons. Soc. for Min., Metall., and Explor., Littleton, CO.

Maniero, R., and P. Canu. 2006. A model of fine particles deposition on smooth surfaces: I. Theoretical basis and model development. Chem. Eng. Sci. 61:7626–7635. doi:10.1016/j.ces.2006.08.064

McCarthy, J.F., and J.M. Zachara. 1989. Subsurface transport of contaminants. Environ. Sci. Technol. 23:496–502.

Mumley, T.E., C.J. Radke, and M.C. Williams. 1986a. Kinetics of liquid/liquid capillary rise: I. Experimental observations. J. Colloid Interface Sci. 109:398–412. doi:10.1016/0021-9797(86)90318-8

Mumley, T.E., C.J. Radke, and M.C. Williams. 1986b. Kinetics of liquid/liquid capillary rise: II. Development and test of theory. J. Colloid Interface Sci. 109:413–425. doi:10.1016/0021-9797(86)90319-X

Nalaskowski, J., A.V. Nguyen, J. Hupka, and J.D. Miller. 2002. Study of particle–bubble interaction using atomic force microscopy: Current possibilities and challenges. Fizykochem. Probl. Mineralurgii 36:253–272.

Nguyen, A.V., and H.J. Schulze. 2004. Colloidal science of flotation. Marcel Dekker, New York.

Noordmans, J., P.J. Wit, H.C. van der Mei, and H.J. Busscher. 1997. Detachment of polystyrene particles from collector surfaces by surface tension forces induced by air-bubble passage through a parallel plate flow chamber. J. Adhes. Sci. Technol. 11:957–969. doi:10.1163/156856197X00525

Ochiai, N., E.L. Kraft, and J.S. Selker. 2006. Methods for colloid transport visualization in pore networks. Water Resour. Res. 42:W12S06. doi:10.1029/2006WR004961

Petkov, J.T., and N.D. Denkov. 2002. Dynamics of particles at interfaces and in thin liquid films. p. 1529–1545. *In* A.T. Hubbard (ed.) Encyclopedia of surface and colloid science. Marcel Dekker, New York.

Pismen, L.M. 2002. Mesoscopic hydrodynamics of contact line motion. Colloids Surf. A 206:11–30. doi:10.1016/S0927-7757(02)00059-6

Pnueli, D., and C. Gutfinger. 1992. Fluid mechanics. Cambridge Univ. Press, Cambridge, UK.

Pomeau, Y. 2002. Recent progress in the moving contact line problem: A review. C.R. Mec. 330:207–222. doi:10.1016/S1631-0721(02)01445-6

Rajagopalan, R., and C. Tien. 1976. Trajectory analysis of deep-bed filtration with the sphere-in-cell porous media model. AIChE J. 22:523–533. doi:10.1002/aic.690220316

Roizard, C., S. Poncin, F. Lapicque, X. Py, and N. Midoux. 1999. Behavior of fine particles in the vicinity of a gas bubble in a stagnant and moving fluid. Chem. Eng. Sci. 54:2317–2323. doi:10.1016/S0009-2509(98)00415-1

Ross, S., and I.D. Morrison. 1988. Colloidal systems and interfaces. John Wiley & Sons, New York.

Russel, W.B., D.A. Saville, and W.R. Schowalter. 1989. Colloidal dispersions. Cambridge Univ. Press, Cambridge, UK.

Saiers, J.E., G.M. Hornberger, D.B. Gower, and J.S. Herman. 2003. The role of moving air–water interfaces in colloid mobilization within the vadose zone. Geophys. Res. Lett. 30(21):2083. doi:10.1029/2003GL018418

Saiers, J.E., and J.J. Lenhart. 2003. Colloid mobilization and transport within unsaturated porous media under transient-flow conditions. Water Resour. Res. 39(1):1019. doi:10.1029/2002WR001370

Saiers, J.E., and J.N. Ryan. 2006. Introduction to special section on colloid transport in subsurface environments. Water Resour. Res. 42:W12S01. doi:10.1029/2006WR005620

Schulze, H.J. 1984. Physico-chemical elementary processes in flotation. Elsevier, Amsterdam.

Sen, T.K., and K.C. Khilar. 2006. Review on subsurface colloids and colloid-associated contaminant transport in saturated porous media. Adv. Colloid Interface Sci. 119:71–96. doi:10.1016/j.cis.2005.09.001

Shang, J., M. Flury, G. Chen, and J. Zhuang. 2008. Impact of flow rate, water content, and capillary forces on in situ colloid mobilization during infiltration in unsaturated sediments. Water Resour. Res. 44:W06411. doi:10.1029/2007WR006516

Shang, J., M. Flury, and Y. Deng. 2009. Force measurements between particles and the air–water interface: Implications for particle mobilization in unsaturated porous media. Water Resour. Res. 45:W06420. doi:10.1029/2008WR007384

Sharma, P., H.M. Abdou, and M. Flury. 2008a. Effect of the lower boundary condition and flotation on colloid mobilization in unsaturated sandy sediments. Vadose Zone J. 7:930–940. doi:10.2136/vzj2007.0163

Sharma, P., M. Flury, and J. Zhou. 2008b. Detachment of colloids from a solid by a moving air–water interface. J. Colloid Interface Sci. 326:143–150. doi:10.1016/j.jcis.2008.07.030

Shen, E.I., and K.S. Udell. 1985. A finite element study of low Reynolds number two-phase flow in cylindrical tubes. J. Appl. Mech. 52:253–256. doi:10.1115/1.3169036

Shi, X., H. Gao, V.I. Lazouskaya, Q. Kang, Y. Jin, and L.-P. Wang. 2010. Viscous flow and colloid transport near air–water interface in a microchannel. Comput. Math. Appl. 59:2290–2304. doi:10.1016/j.camwa.2009.08.059

Shikhmurzaev, Y.D. 2006. Singularities at the moving contact line: Mathematical, physical and computational aspects. Physica D 217:121–133. doi:10.1016/j.physd.2006.03.003

Sirivithayapakorn, S., and A. Keller. 2003a. Transport of colloids in saturated porous media: A pore-scale observation of the size exclusion effect and colloid acceleration. Water Resour. Res. 39:1109. doi:10.1029/2002WR001583

Sirivithayapakorn, S., and A. Keller. 2003b. Transport of colloids in unsaturated porous media: A pore-scale observation of processes during the dissolution of air–water interface. Water Resour. Res. 39(12):1346. doi:10.1029/2003WR002487

Spielman, L.A. 1977. Particle capture from low-speed laminar flows. Annu. Rev. Fluid Mech. 9:297–319. doi:10.1146/annurev.fl.09.010177.001501

Spielman, L.A., and S.L. Goren. 1970. Capture of small particles by London forces from low-speed liquid flows. Environ. Sci. Technol. 4:135–140. doi:10.1021/es60037a007

Steenhuis, T.S., J.F. McCarthy, J.T. Crist, Y. Zevi, P.C. Baveye, J.A. Throop, R.L. Fehrman, A. Dathe, and B.K. Richards. 2005. Reply to "Comments on 'Pore-scale visualization of colloid transport and retention in partly saturated porous media.' " Vadose Zone J. 4:957–958. doi:10.2136/vzj2005.0041

Taha, T., and Z.F. Cui. 2006. CFD modelling of slug flow inside square capillaries. Chem. Eng. Sci. 61:665–675. doi:10.1016/j.ces.2005.07.023

Torkzaban, S., S.A. Bradford, M.Th. van Genuchten, and S.L. Walker. 2008. Colloid transport in unsaturated porous media: The role of water content and ionic strength on particle straining. J. Contam. Hydrol. 96:113–127. doi:10.1016/j.jconhyd.2007.10.006

Torkzaban, S., S.A. Bradford, and S.L. Walker. 2007. Resolving the coupled effects of hydrodynamics and DLVO forces on colloid attachment in porous media. Langmuir 23:9652–9660. doi:10.1021/la700995e

Verwey, E.J.W., and J.Th.G. Overbeek. 1948. Theory of the stability of lyophobic colloids. Elsevier, New York.

Wan, J., and T.K. Tokunaga. 1997. Film straining of colloids in unsaturated porous media: Conceptual model and experimental testing. Environ. Sci. Technol. 31:2413–2420. doi:10.1021/es970017q

Wan, J., and T.K. Tokunaga. 2005. Comments on "Pore-scale visualization of colloid transport and retention in partly saturated porous media." Vadose Zone J. 4:954–956. doi:10.2136/vzj2005.0010

Wan, J., and J.L. Wilson. 1992. Colloid transport and the gas–water interface in porous media. p. 55–70. *In* D.A. Sabatini and R.C. Knox (ed.) Transport and remediation of subsurface contaminants: Colloidal, interfacial, and surfactant phenomena. Am. Chem. Soc., Washington, DC.

Wan, J., and J.L. Wilson. 1993. Visualization of colloid transport during single and two-fluid flow in porous media. p. 335–339. *In* J.F. McCarthy and F.J. Wobber (ed.) Manipulation of groundwater colloids for environmental restoration. CRC Press, Boca Raton, FL.

Wan, J., and J.L. Wilson. 1994. Visualization of the role of the gas–water interface on the fate and transport of colloids in porous media. Water Resour. Res. 30:11–23. doi:10.1029/93WR02403

Wan, J., J.L. Wilson, and T.L. Kieft. 1994. Influence of the gas–water interface on transport of microorganisms through unsaturated porous media. Appl. Environ. Microbiol. 60:509–516.

Warszynski, P. 2000. Coupling of hydrodynamic and electric interactions in adsorption of colloidal particles. Adv. Colloid Interface Sci. 84:47–142. doi:10.1016/S0001-8686(99)00015-9

Wiesner, M.R., G.V. Lowry, P. Alvarez, D. Dionysiou, and P. Bismas. 2006. Assessing the risks of manufactured nanomaterials. Environ. Sci. Technol. 40:4336–4345. doi:10.1021/es062726m

Yamaguchi, E., B.J. Smith, and D.P. Gaver III. 2009. μ-PIV measurements of the ensemble flow fields surrounding a migrating semi-infinite bubble. Exp. Fluids 47:309–320. doi:10.1007/s00348-009-0662-1

Yao, K.-M., M.T. Habibian, and C.R. O'Melia. 1971. Water and waste water filtration: Concepts and applications. Environ. Sci. Technol. 5:1105–1112. doi:10.1021/es60058a005

Yoon, R.-H., and L. Mao. 1996. Application of extended DLVO theory: IV. Derivation of flotation rate equation from first principles. J. Colloid Interface Sci. 181:613–626. doi:10.1006/jcis.1996.0419

Zevi, Y., A. Dathe, J.F. McCarthy, B.K. Richards, and T.S. Steenhuis. 2005. Distribution of colloid particles onto interfaces in partially saturated sand. Environ. Sci. Technol. 39:7055–7064. doi:10.1021/es048595b

Zhuang, J., J.F. McCarthy, J.S. Tyner, E. Perfect, and M. Flury. 2007. In situ colloid mobilization in Hanford sediments under unsaturated transient flow conditions: Effect of irrigation pattern. Environ. Sci. Technol. 41:3199–3204. doi:10.1021/es062757h